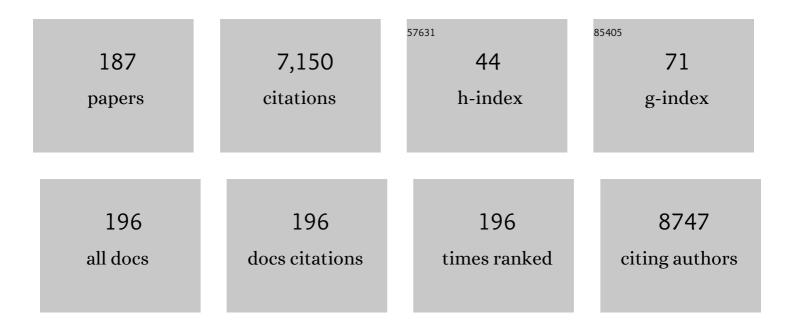
Xiao-Long Liu

List of Publications by Year in descending order

Source: https://exaly.com/author-pdf/3878224/publications.pdf Version: 2024-02-01



#	Article	IF	CITATIONS
1	Synthetic Biology in Chimeric Antigen Receptor T (CAR T) Cell Engineering. ACS Synthetic Biology, 2022, 11, 1-15.	1.9	14
2	Tracking Cell Viability for Adipose-Derived Mesenchymal Stem Cell-Based Therapy by Quantitative Fluorescence Imaging in the Second Near-Infrared Window. ACS Nano, 2022, 16, 2889-2900.	7.3	22
3	Copy number profiling of circulating free DNA predicts transarterial chemoembolization response in advanced hepatocellular carcinoma. Molecular Oncology, 2022, 16, 1986-1999.	2.1	4
4	CD16/PD-L1 bi-specific aptamer for cancer immunotherapy through recruiting NK cells and acting as immunocheckpoint blockade. Molecular Therapy - Nucleic Acids, 2022, 27, 998-1009.	2.3	10
5	Neoantigen Immunotherapeutic-Gel Combined with TIM-3 Blockade Effectively Restrains Orthotopic Hepatocellular Carcinoma Progression. Nano Letters, 2022, 22, 2048-2058.	4.5	17
6	Nanoplatform Selfâ€Assembly from Small Molecules of Porphyrin Derivatives for NIRâ€II Fluorescence Imaging Guided Photothermalâ€Immunotherapy. Advanced Healthcare Materials, 2022, 11, e2102526.	3.9	18
7	Red Blood Cell-Mimic Nanocatalyst Triggering Radical Storm to Augment Cancer Immunotherapy. Nano-Micro Letters, 2022, 14, 57.	14.4	24
8	Far-Red Light Triggered Production of Bispecific T Cell Engagers (BiTEs) from Engineered Cells for Antitumor Application. ACS Synthetic Biology, 2022, , .	1.9	1
9	Surface-Engineered Gold Nanoclusters for Stimulated Emission Depletion and Correlated Light and Electron Microscopy Imaging. Analytical Chemistry, 2022, 94, 3056-3064.	3.2	22
10	Remodeling Tumorâ€Associated Neutrophils to Enhance Dendritic Cellâ€Based HCC Neoantigen Nanoâ€Vaccine Efficiency. Advanced Science, 2022, 9, e2105631.	5.6	51
11	Exploiting Photoelectric Activities and Piezoelectric Properties of NaNbO ₃ Semiconductors for Point-of-Care Immunoassay. Analytical Chemistry, 2022, 94, 3418-3426.	3.2	151
12	Biodegradable Nanoprobe for NIRâ€ I I Fluorescence Imageâ€Guided Surgery and Enhanced Breast Cancer Radiotherapy Efficacy. Advanced Science, 2022, 9, e2104728.	5.6	35
13	Liposome-Mediated <i>In Situ</i> Formation of Type-I Heterojunction for Amplified Photoelectrochemical Immunoassay. Analytical Chemistry, 2022, 94, 4859-4865.	3.2	176
14	Development and evaluation of a new test kit for determination of immunosuppressants in blood by UHPLC-MS/MS. Journal of Pharmaceutical and Biomedical Analysis, 2022, 215, 114756.	1.4	0
15	Natural Killer Cell Membraneâ€Cloaked Virusâ€Mimicking Nanogenerator with NIRâ€Triggered Shape Reversal and •C/•OH Storm for Synergistic Thermodynamic–Chemodynamic Therapy. Advanced Science, 2022, 9, e2103498.	5.6	29
16	Tumor Microenvironment-Responsive Yolk–Shell NaCl@Virus-Inspired Tetrasulfide-Organosilica for Ion-Interference Therapy <i>via</i> Osmolarity Surge and Oxidative Stress Amplification. ACS Nano, 2022, 16, 7380-7397.	7.3	25
17	Gold-seaurchin based immunomodulator enabling photothermal intervention and αCD16 transfection to boost NK cell adoptive immunotherapy. Acta Biomaterialia, 2022, 146, 406-420.	4.1	9
18	Liposome-Embedded Cu _{2–<i>x</i>} Ag _{<i>x</i>} S Nanoparticle-Mediated Photothermal Immunoassay for Daily Monitoring of cTnI Protein Using a Portable Thermal Imager. Analytical Chemistry, 2022, 94, 7408-7416.	3.2	61

#	Article	IF	CITATIONS
19	Biosynthetic cell membrane vesicles to enhance TRAIL-mediated apoptosis driven by photo-triggered oxidative stress. Biomaterials Science, 2022, 10, 3547-3558.	2.6	3
20	Integrated Photothermalâ€Pyroelectric Biosensor for Rapid and Pointâ€ofâ€Care Diagnosis of Acute Myocardial Infarction: A Convergence of Theoretical Research and Commercialization. Small, 2022, 18,	5.2	28
21	Comparison of sample preparation methods, validation of an UPLC–MS/MS procedure for the quantification of cyclosporine A in whole blood sample. Journal of Pharmaceutical and Biomedical Analysis, 2021, 193, 113672.	1.4	3
22	A novel long-wavelength off-on fluorescence probe for nitroreductase analysis and hypoxia imaging. Analytica Chimica Acta, 2021, 1144, 76-84.	2.6	15
23	CRISPR-Cas12a coupled with terminal deoxynucleotidyl transferase mediated isothermal amplification for sensitive detection of polynucleotide kinase activity. Sensors and Actuators B: Chemical, 2021, 330, 129317.	4.0	22
24	Profiling of hepatocellular carcinoma neoantigens reveals immune microenvironment and clonal evolution related patterns. Chinese Journal of Cancer Research: Official Journal of China Anti-Cancer Association, Beijing Institute for Cancer Research, 2021, 33, 364-378.	0.7	11
25	A remotely controlled NIR-II photothermal-sensitive transgene system for hepatocellular carcinoma synergistic therapy. Journal of Materials Chemistry B, 2021, 9, 5083-5091.	2.9	13
26	Localized NIR-II photo-immunotherapy through the combination of photothermal ablation and <i>in situ</i> generated interleukin-12 cytokine for efficiently eliminating primary and abscopal tumors. Nanoscale, 2021, 13, 1745-1758.	2.8	32
27	Cytosolic Delivery of Thiolated Neoantigen Nanoâ€Vaccine Combined with Immune Checkpoint Blockade to Boost Anti ancer T Cell Immunity. Advanced Science, 2021, 8, 2003504.	5.6	34
28	Redirecting natural killer cells to potentiate adoptive immunotherapy in solid tumors through stabilized Y-type bispecific aptamer. Nanoscale, 2021, 13, 11279-11288.	2.8	11
29	Enhancing therapeutic effects and <i>in vivo</i> tracking of adipose tissue-derived mesenchymal stem cells for liver injury using bioorthogonal click chemistry. Nanoscale, 2021, 13, 1813-1822.	2.8	13
30	A highly stable multifunctional aptamer for enhancing antitumor immunity against hepatocellular carcinoma by blocking dual immune checkpoints. Biomaterials Science, 2021, 9, 4159-4168.	2.6	18
31	Tumor Microenvironment Triggered Cascadeâ€Activation Nanoplatform for Synergistic and Precise Treatment of Hepatocellular Carcinoma. Advanced Healthcare Materials, 2021, 10, e2002036.	3.9	14
32	Genome-scale profiling of circulating cell-free DNA signatures for early detection of hepatocellular carcinoma in cirrhotic patients. Cell Research, 2021, 31, 589-592.	5.7	59
33	Quantitative Secretome Analysis Reveals Clinical Values of Carbonic Anhydrase II in Hepatocellular Carcinoma. Genomics, Proteomics and Bioinformatics, 2021, 19, 94-107.	3.0	6
34	Cytosolic Delivery of Thiolated Mn GAMP Nanovaccine to Enhance the Antitumor Immune Responses. Small, 2021, 17, e2006970.	5.2	38
35	Emerging nanotechnological strategies to reshape tumor microenvironment for enhanced therapeutic outcomes of cancer immunotherapy. Biomedical Materials (Bristol), 2021, 16, 042001.	1.7	6
36	Development of Prognostic Evaluation Model to Predict the Overall Survival and Early Recurrence of Hepatocellular Carcinoma. Journal of Hepatocellular Carcinoma, 2021, Volume 8, 301-312.	1.8	1

#	Article	IF	CITATIONS
37	Growing Human Hepatocellular Tumors Undergo a Global Metabolic Reprogramming. Cancers, 2021, 13, 1980.	1.7	9
38	The Landscape of Cell-Free HBV Integrations and Mutations in Cirrhosis and Hepatocellular Carcinoma Patients. Clinical Cancer Research, 2021, 27, 3772-3783.	3.2	21
39	Virus-like mesoporous silica-coated plasmonic Ag nanocube with strong bacteria adhesion for diabetic wound ulcer healing. Nanomedicine: Nanotechnology, Biology, and Medicine, 2021, 34, 102381.	1.7	22
40	Accurate transcriptome assembly by Nanopore RNA sequencing reveals novel functional transcripts in hepatocellular carcinoma. Cancer Science, 2021, 112, 3555-3568.	1.7	6
41	Hypoxia-responsive nanoreactors based on self-enhanced photodynamic sensitization and triggered ferroptosis for cancer synergistic therapy. Journal of Nanobiotechnology, 2021, 19, 204.	4.2	36
42	A combined Cox and logistic model provides accurate predictive performance in estimation of time-dependent probabilities for recurrence of intrahepatic cholangiocarcinoma after resection. Hepatobiliary Surgery and Nutrition, 2021, 10, 464-475.	0.7	7
43	In Vivo Tracking of Cell Viability for Adoptive Natural Killer Cellâ€Based Immunotherapy by Ratiometric NIRâ€II Fluorescence Imaging. Angewandte Chemie, 2021, 133, 21056-21064.	1.6	10
44	In Vivo Tracking of Cell Viability for Adoptive Natural Killer Cellâ€Based Immunotherapy by Ratiometric NIRâ€II Fluorescence Imaging. Angewandte Chemie - International Edition, 2021, 60, 20888-20896.	7.2	48
45	Chemiluminescence-Derived Self-Powered Photoelectrochemical Immunoassay for Detecting a Low-Abundance Disease-Related Protein. Analytical Chemistry, 2021, 93, 13389-13397.	3.2	118
46	Sustained Antitumor Immunity Based on Persistent Luminescence Nanoparticles for Cancer Immunotherapy. Advanced Functional Materials, 2021, 31, 2106884.	7.8	21
47	Pressure-Based Immunoassays with Versatile Electronic Sensors for Carcinoembryonic Antigen Detection. ACS Applied Materials & Interfaces, 2021, 13, 46440-46450.	4.0	34
48	Chiral Hybrid Perovskite Single rystal Nanowire Arrays for Highâ€Performance Circularly Polarized Light Detection. Advanced Science, 2021, 8, e2102065.	5.6	34
49	Low-dose exposure to black carbon significantly increase lung injury of cadmium by promoting cellular apoptosis. Ecotoxicology and Environmental Safety, 2021, 224, 112703.	2.9	11
50	CRISPR/Cas12a-mediated liposome-amplified strategy for the photoelectrochemical detection of nucleic acid. Chemical Communications, 2021, 57, 8977-8980.	2.2	87
51	Pressure-Based Biosensor Integrated with a Flexible Pressure Sensor and an Electrochromic Device for Visual Detection. Analytical Chemistry, 2021, 93, 2916-2925.	3.2	181
52	Engineered Red Blood Cell Biomimetic Nanovesicle with Oxygen Self-Supply for Near-Infrared-II Fluorescence-Guided Synergetic Chemo-Photodynamic Therapy against Hypoxic Tumors. ACS Applied Materials & Interfaces, 2021, 13, 52435-52449.	4.0	34
53	Thermally Activated Lasing in Organic Microcrystals toward Laser Displays. Journal of the American Chemical Society, 2021, 143, 20249-20255.	6.6	29
54	Personalized neoantigen vaccine prevents postoperative recurrence in hepatocellular carcinoma patients with vascular invasion. Molecular Cancer, 2021, 20, 164.	7.9	44

#	Article	IF	CITATIONS
55	An integrative pan-cancer analysis of biological and clinical impacts underlying ubiquitin-specific-processing proteases. Oncogene, 2020, 39, 587-602.	2.6	11
56	Rapid and highly sensitive quantification of the anti-tuberculosis agents isoniazid, ethambutol, pyrazinamide, rifampicin and rifabutin in human plasma by UPLC-MS/MS. Journal of Pharmaceutical and Biomedical Analysis, 2020, 180, 113076.	1.4	16
57	Donor–acceptor conjugated polymer-based nanoparticles for highly effective photoacoustic imaging and photothermal therapy in the NIR-II window. Chemical Communications, 2020, 56, 1093-1096.	2.2	63
58	Protein-assisted formation of gold clusters-MnO2 nanocomposite for fluorescence imaging of intracellular glutathione. Talanta, 2020, 209, 120524.	2.9	18
59	Photodynamic Therapy Combined with Antihypoxic Signaling and CpG Adjuvant as an In Situ Tumor Vaccine Based on Metal–Organic Framework Nanoparticles to Boost Cancer Immunotherapy. Advanced Healthcare Materials, 2020, 9, e1900996.	3.9	117
60	Ku80 negatively regulates the expression of OCT4 via competitive binding to SALL4 and promoting lysosomal degradation of OCT4. International Journal of Biochemistry and Cell Biology, 2020, 118, 105664.	1.2	3
61	Surface modification of TiO2 nanosheets with fullerene and zinc-phthalocyanine for enhanced photocatalytic reduction under solar-light irradiation. Science China Materials, 2020, 63, 2251-2260.	3.5	15
62	Ultrasound-Driven Biomimetic Nanosystem Suppresses Tumor Growth and Metastasis through Sonodynamic Therapy, CO Therapy, and Indoleamine 2,3-Dioxygenase Inhibition. ACS Nano, 2020, 14, 8985-8999.	7.3	82
63	Mesenchymal stromal cell therapies: immunomodulatory properties and clinical progress. Stem Cell Research and Therapy, 2020, 11, 345.	2.4	158
64	Cancer Cell-Targeted Photosensitizer and Therapeutic Protein Co-Delivery Nanoplatform Based on a Metal–Organic Framework for Enhanced Synergistic Photodynamic and Protein Therapy. ACS Applied Materials & Interfaces, 2020, 12, 36906-36916.	4.0	58
65	Molecularly Engineered Strong Metal Oxide–Support Interaction Enables Highly Efficient and Stable CO ₂ Electroreduction. ACS Catalysis, 2020, 10, 13227-13235.	5.5	94
66	A near-infrared turn-on fluorescence probe for glutathione detection based on nanocomposites of semiconducting polymer dots and MnO2 nanosheets. Analytical and Bioanalytical Chemistry, 2020, 412, 8167-8176.	1.9	13
67	Tumor Microenvironment Cascade-Responsive Nanodrug with Self-Targeting Activation and ROS Regeneration for Synergistic Oxidation-Chemotherapy. Nano-Micro Letters, 2020, 12, 182.	14.4	38
68	A thieno-isoindigo derivative-based conjugated polymer nanoparticle for photothermal therapy in the NIR-II bio-window. Nanoscale, 2020, 12, 19665-19672.	2.8	34
69	Platinum Nanozyme-Triggered Pressure-Based Immunoassay Using a Three-Dimensional Polypyrrole Foam-Based Flexible Pressure Sensor. ACS Applied Materials & Interfaces, 2020, 12, 40133-40140.	4.0	123
70	An immune checkpoint score system for prognostic evaluation and adjuvant chemotherapy selection in gastric cancer. Nature Communications, 2020, 11, 6352.	5.8	67
71	An Isothermal Method for Sensitive Detection of Mycobacterium tuberculosis Complex Using Clustered Regularly Interspaced Short Palindromic Repeats/Cas12a Cis and Trans Cleavage. Journal of Molecular Diagnostics, 2020, 22, 1020-1029.	1.2	27
72	Proteomic analyses reveal divergent ubiquitylation patterns in hepatocellula carcinoma cell lines with different metastasis potential. Journal of Proteomics, 2020, 225, 103834.	1.2	9

#	Article	IF	CITATIONS
73	Self-assembled metallo-supramolecular nanoflowers for NIR/acidic-triggered multidrug release, long-term tumor retention and NIR-II fluorescence imaging-guided photo-chemotherapy. Chemical Engineering Journal, 2020, 400, 125882.	6.6	30
74	Antioxidant preconditioning improves therapeutic outcomes of adipose tissue-derived mesenchymal stem cells through enhancing intrahepatic engraftment efficiency in a mouse liver fibrosis model. Stem Cell Research and Therapy, 2020, 11, 237.	2.4	30
75	<p>Not All Hepatocellular Carcinoma Patients with Microvascular Invasion After RO Resection Could Be Benefited from Prophylactic Transarterial Chemoembolization: A Propensity Score Matching Study</p> . Cancer Management and Research, 2020, Volume 12, 3815-3825.	0.9	14
76	Wettabilityâ€Guided Screen Printing of Perovskite Microlaser Arrays for Currentâ€Driven Displays. Advanced Materials, 2020, 32, e2001999.	11.1	66
77	Genomic and Transcriptomic Landscape of Tumor Clonal Evolution in Cholangiocarcinoma. Frontiers in Genetics, 2020, 11, 195.	1.1	4
78	Equipping Natural Killer Cells with Specific Targeting and Checkpoint Blocking Aptamers for Enhanced Adoptive Immunotherapy in Solid Tumors. Angewandte Chemie - International Edition, 2020, 59, 12022-12028.	7.2	114
79	HIF-1α and HDAC1 mediated regulation of FAM99A-miR92a signaling contributes to hypoxia induced HCC metastasis. Signal Transduction and Targeted Therapy, 2020, 5, 118.	7.1	25
80	Converting Immune Cold into Hot by Biosynthetic Functional Vesicles to Boost Systematic Antitumor Immunity. IScience, 2020, 23, 101341.	1.9	34
81	In Situ Switching of Photoinduced Electron Transfer Direction by Regulating the Redox State in Fullerene-Based Dyads. Journal of the American Chemical Society, 2020, 142, 4411-4418.	6.6	31
82	Moesin facilitates metastasis of hepatocellular carcinoma cells by improving invadopodia formation and activating β-catenin/MMP9 axis. Biochemical and Biophysical Research Communications, 2020, 524, 861-868.	1.0	15
83	Tumor microenvironment-activated self-recognizing nanodrug through directly tailored assembly of small-molecules for targeted synergistic chemotherapy. Journal of Controlled Release, 2020, 321, 222-235.	4.8	72
84	Hepatic fibrinogen storage disease and hypofibrinogenemia caused by fibrinogen Aguadilla mutation: a case report. Journal of International Medical Research, 2020, 48, 030006051989803.	0.4	7
85	RBC Membrane Camouflaged Semiconducting Polymer Nanoparticles for Near-Infrared Photoacoustic Imaging and Photothermal Therapy. Nano-Micro Letters, 2020, 12, 94.	14.4	60
86	Equipping Natural Killer Cells with Specific Targeting and Checkpoint Blocking Aptamers for Enhanced Adoptive Immunotherapy in Solid Tumors. Angewandte Chemie, 2020, 132, 12120-12126.	1.6	17
87	Personalized neoantigen-based immunotherapy for advanced collecting duct carcinoma: case report. , 2020, 8, e000217.		18
88	Deathâ€associated protein kinase 1 suppresses hepatocellular carcinoma cell migration and invasion by upregulation of DEADâ€box helicase 20. Cancer Science, 2020, 111, 2803-2813.	1.7	13
89	Lead-free thermochromic perovskites with tunable transition temperatures for smart window applications. Science China Chemistry, 2019, 62, 1257-1262.	4.2	39
90	Sensitive fluorometric determination of glutathione using fluorescent polymer dots and the dopamine-melanin nanosystem. Mikrochimica Acta, 2019, 186, 568.	2.5	9

#	Article	IF	CITATIONS
91	Periodicity of Quadrilateral Tetra-Atomic Molecules. Journal of Physical Chemistry A, 2019, 123, 6652-6659.	1.1	1
92	Water-soluble organic probe for pH sensing and imaging. Talanta, 2019, 205, 120095.	2.9	23
93	Dual sensing of glutathione and acidic pH values by using MnO2 nanosheets and 3-acetyl-7-hydroxy-2H-chromen-2-one as a fluorescent pH probe. Mikrochimica Acta, 2019, 186, 491.	2.5	8
94	Tumor Microenvironment Responsive Shape-Reversal Self-Targeting Virus-Inspired Nanodrug for Imaging-Guided Near-Infrared-II Photothermal Chemotherapy. ACS Nano, 2019, 13, 12912-12928.	7.3	118
95	Artificial Engineered Natural Killer Cells Combined with Antiheat Endurance as a Powerful Strategy for Enhancing Photothermalâ€Immunotherapy Efficiency of Solid Tumors. Small, 2019, 15, e1902636.	5.2	43
96	Antioxidants inhibit cell senescence and preserve stemness of adipose tissue-derived stem cells by reducing ROS generation during long-term in vitro expansion. Stem Cell Research and Therapy, 2019, 10, 306.	2.4	71
97	Dataset for quantitative phospho-proteomics analysis of a serial hepatoma cell lines with increasing invasion and metastasis potential. Data in Brief, 2019, 27, 104634.	0.5	0
98	Immunotherapy: Artificial Engineered Natural Killer Cells Combined with Antiheat Endurance as a Powerful Strategy for Enhancing Photothermalâ€Immunotherapy Efficiency of Solid Tumors (Small) Tj ETQq0 0 0	rg∰2 /Ov€	erl ac k 10 Tf 5
99	Developing IR-780 as a Novel Matrix for Enhanced MALDI MS Imaging of Endogenous High-Molecular-Weight Lipids in Brain Tissues. Analytical Chemistry, 2019, 91, 15873-15882.	3.2	18
100	Tuning wettability of molten lithium via a chemical strategy for lithium metal anodes. Nature Communications, 2019, 10, 4930.	5.8	181
101	Highly efficient redox reaction between potassium permanganate and 3,3′,5,5′-tetramethylbenzidine for application in hydrogen peroxide based colorimetric assays. RSC Advances, 2019, 9, 1889-1894.	1.7	12
102	The biobehavior, biocompatibility and theranostic application of SPNS and Pd@Au nanoplates in rats and rabbits. Chemical Science, 2019, 10, 1677-1686.	3.7	18
103	<p>The serum proteomics tracking of hepatocellular carcinoma early recurrence following radical resection</p> . Cancer Management and Research, 2019, Volume 11, 2935-2946.	0.9	20
104	Comprehensive Liquid Profiling of Circulating Tumor DNA and Protein Biomarkers in Long-Term Follow-Up Patients with Hepatocellular Carcinoma. Clinical Cancer Research, 2019, 25, 5284-5294.	3.2	90
105	Folic acid-conjugated gold nanorod@polypyrrole@Fe3O4 nanocomposites for targeted MR/CT/PA multimodal imaging and chemo-photothermal therapy. RSC Advances, 2019, 9, 18874-18887.	1.7	13
106	Application of PD-1 Blockade in Cancer Immunotherapy. Computational and Structural Biotechnology Journal, 2019, 17, 661-674.	1.9	333
107	Prognostic Value of MicroRNA-497 in Various Cancers: A Systematic Review and Meta-Analysis. Disease Markers, 2019, 2019, 1-9.	0.6	11
108	Nearâ€Infrared Light Activated Thermosensitive Ion Channel to Remotely Control Transgene System for Thrombolysis Therapy. Small, 2019, 15, e1901176.	5.2	17

#	Article	lF	CITATIONS
109	An Optogenetic Controllable T Cell System for Hepatocellular Carcinoma Immunotherapy. Theranostics, 2019, 9, 1837-1850.	4.6	33
110	Highly photoluminescent and temperature-sensitive P,ÂN, B-co-doped carbon quantum dots and their highly sensitive recognition for curcumin. RSC Advances, 2019, 9, 8340-8349.	1.7	31
111	ANXA2Tyr23 and FLNASer2152 phosphorylation associate with poor prognosis in hepatic carcinoma revealed by quantitative phosphoproteomics analysis. Journal of Proteomics, 2019, 200, 111-122.	1.2	16
112	Programmable Therapeutic Nanodevices with Circular Amplification of H ₂ O ₂ in the Tumor Microenvironment for Synergistic Cancer Therapy. Advanced Healthcare Materials, 2019, 8, e1801627.	3.9	27
113	The design of Janus black phosphorus quantum dots@metal–organic nanoparticles for simultaneously enhancing environmental stability and photodynamic therapy efficiency. Materials Chemistry Frontiers, 2019, 3, 656-663.	3.2	19
114	<p>FGG promotes migration and invasion in hepatocellular carcinoma cells through activating epithelial to mesenchymal transition</p> . Cancer Management and Research, 2019, Volume 11, 1653-1665.	0.9	28
115	Photocatalysis Enhancement for Programmable Killing of Hepatocellular Carcinoma through Self-Compensation Mechanisms Based on Black Phosphorus Quantum-Dot-Hybridized Nanocatalysts. ACS Applied Materials & Interfaces, 2019, 11, 9804-9813.	4.0	63
116	A novel empirical method for quickly estimating the charge-transfer state of fullerene-donor derivatives. Physical Chemistry Chemical Physics, 2019, 21, 24291-24295.	1.3	4
117	Self-Luminescing Theranostic Nanoreactors with Intraparticle Relayed Energy Transfer for Tumor Microenvironment Activated Imaging and Photodynamic Therapy. Theranostics, 2019, 9, 20-33.	4.6	53
118	Genomic and transcriptional Profiling of tumor infiltrated CD8 ⁺ T cells revealed functional heterogeneity of antitumor immunity in hepatocellular carcinoma. OncoImmunology, 2019, 8, e1538436.	2.1	17
119	Metabolomics profiling of metformin-mediated metabolic reprogramming bypassing AMPKα. Metabolism: Clinical and Experimental, 2019, 91, 18-29.	1.5	30
120	Polydopamine doped reduced graphene oxide/mesoporous silica nanosheets for chemo-photothermal and enhanced photothermal therapy. Materials Science and Engineering C, 2019, 96, 138-145.	3.8	46
121	Integrating phosphoproteomics into kinase-targeted cancer therapies in precision medicine. Journal of Proteomics, 2019, 191, 68-79.	1.2	30
122	Localized Surface Plasmon Resonance Enhanced Singlet Oxygen Generation and Light Absorption Based on Black Phosphorus@AuNPs Nanosheet for Tumor Photodynamic/Thermal Therapy. Particle and Particle Systems Characterization, 2018, 35, 1800010.	1.2	39
123	Polydopamine-assisted versatile modification of a nucleic acid probe for intracellular microRNA imaging and enhanced photothermal therapy. RSC Advances, 2018, 8, 6781-6788.	1.7	7
124	Gadolinium-doped hollow CeO ₂ -ZrO ₂ nanoplatform as multifunctional MRI/CT dual-modal imaging agent and drug delivery vehicle. Drug Delivery, 2018, 25, 353-363.	2.5	14
125	Chemotherapeutic Drug Based Metal–Organic Particles for Microvesicleâ€Mediated Deep Penetration and Programmable pH/NIR/Hypoxia Activated Cancer Photochemotherapy. Advanced Science, 2018, 5, 1700648.	5.6	60
126	Reduction/photo dual-responsive polymeric prodrug nanoparticles for programmed siRNA and doxorubicin delivery. Biomaterials Science, 2018, 6, 1457-1468.	2.6	51

#	Article	IF	CITATIONS
127	Semiconducting polymer-based nanoparticles for photothermal therapy at the second near-infrared window. Chemical Communications, 2018, 54, 13599-13602.	2.2	47
128	One-pot synthesis of biodegradable polydopamine-doped mesoporous silica nanocomposites (PMSNs) as pH-sensitive targeting drug nanocarriers for synergistic chemo-photothermal therapy. RSC Advances, 2018, 8, 37433-37440.	1.7	18
129	Facile preparation of biocompatible Ti ₂ O ₃ nanoparticles for second near-infrared window photothermal therapy. Journal of Materials Chemistry B, 2018, 6, 7889-7897.	2.9	25
130	A MnO ₂ nanosheets– <i>o</i> -phenylenediamine oxidative system for the sensitive fluorescence determination of alkaline phosphatase activity. Analytical Methods, 2018, 10, 5341-5346.	1.3	10
131	Suppressing Nonradiative Processes of Organic Dye with Metal–Organic Framework Encapsulation toward Near-Infrared Solid-State Microlasers. ACS Applied Materials & Interfaces, 2018, 10, 35455-35461.	4.0	33
132	A novel transcription factor Rwdd1 and its SUMOylation inhibit the expression of sqr, a key gene of mitochondrial sulfide metabolism in Urechis unicinctus. Aquatic Toxicology, 2018, 204, 180-189.	1.9	8
133	Clonal evolution in longâ€ŧerm followâ€up patients with hepatocellular carcinoma. International Journal of Cancer, 2018, 143, 2862-2870.	2.3	18
134	Photoresponsive Nanovehicle for Two Independent Wavelength Light-Triggered Sequential Release of P-gp shRNA and Doxorubicin To Optimize and Enhance Synergistic Therapy of Multidrug-Resistant Cancer. ACS Applied Materials & Interfaces, 2018, 10, 19416-19427.	4.0	67
135	Hyperspectral Stimulated Raman Scattering Microscopy Unravels Aberrant Accumulation of Saturated Fat in Human Liver Cancer. Analytical Chemistry, 2018, 90, 6362-6366.	3.2	48
136	Photo-responsive hollow silica nanoparticles for light-triggered genetic and photodynamic synergistic therapy. Acta Biomaterialia, 2018, 76, 178-192.	4.1	30
137	Comparative proteomics of side population cells derived from human hepatocellular carcinoma cell lines with varying metastatic potentials. Oncology Letters, 2018, 16, 335-345.	0.8	8
138	pH/hypoxia programmable triggered cancer photo-chemotherapy based on a semiconducting polymer dot hybridized mesoporous silica framework. Chemical Science, 2018, 9, 7390-7399.	3.7	59
139	USP10 suppresses tumor progression by inhibiting mTOR activation in hepatocellular carcinoma. Cancer Letters, 2018, 436, 139-148.	3.2	49
140	Self-Quenched Metal–Organic Particles as Dual-Mode Therapeutic Agents for Photoacoustic Imaging-Guided Second Near-Infrared Window Photochemotherapy. ACS Applied Materials & Interfaces, 2018, 10, 25203-25212.	4.0	63
141	Cancer cell membrane-coated magnetic nanoparticles for MR/NIR fluorescence dual-modal imaging and photodynamic therapy. Biomaterials Science, 2018, 6, 1834-1845.	2.6	88
142	Cationic nanomicelles derived from Pluronic F127 as delivery vehicles of Chinese herbal medicine active components of ursolic acid for colorectal cancer treatment. RSC Advances, 2018, 8, 15906-15914.	1.7	12
143	Light-Enhanced Hypoxia-Response of Conjugated Polymer Nanocarrier for Successive Synergistic Photodynamic and Chemo-Therapy. ACS Applied Materials & Interfaces, 2018, 10, 21909-21919.	4.0	73
144	Hybrid Three-Dimensional Spiral WSe ₂ Plasmonic Structures for Highly Efficient Second-Order Nonlinear Parametric Processes. Research, 2018, 2018, 4164029.	2.8	15

#	Article	IF	CITATIONS
145	Tumor Microenvironment Activable Selfâ€Assembled DNA Hybrids for pH and Redox Dualâ€Responsive Chemotherapy/PDT Treatment of Hepatocellular Carcinoma. Advanced Science, 2017, 4, 1600460.	5.6	56
146	Photoresponsive lipid-polymer hybrid nanoparticles for controlled doxorubicin release. Nanotechnology, 2017, 28, 255101.	1.3	27
147	Circulating tumor DNA profiling reveals clonal evolution and realâ€time disease progression in advanced hepatocellular carcinoma. International Journal of Cancer, 2017, 141, 977-985.	2.3	71
148	A fluorescence sensing platform with the MnO2 nanosheets as an effective oxidant for glutathione detection. Sensors and Actuators B: Chemical, 2017, 252, 30-36.	4.0	39
149	Facile synthesis of multifunctional Fe ₃ O ₄ @SiO ₂ @Au magneto-plasmonic nanoparticles for MR/CT dual imaging and photothermal therapy. RSC Advances, 2017, 7, 18844-18850.	1.7	40
150	A fluorescence based immunoassay for galectin-4 using gold nanoclusters and a composite consisting of glucose oxidase and a metal-organic framework. Mikrochimica Acta, 2017, 184, 1933-1940.	2.5	29
151	Magnetite nanocluster and paclitaxel-loaded charge-switchable nanohybrids for MR imaging and chemotherapy. Journal of Materials Chemistry B, 2017, 5, 849-857.	2.9	18
152	A fluorescent turn on nanoprobe for simultaneous visualization of dual-targets involved in cell apoptosis and drug screening in living cells. Nanoscale, 2017, 9, 10861-10868.	2.8	28
153	Glutathione responsive micelles incorporated with semiconducting polymer dots and doxorubicin for cancer photothermal-chemotherapy. Nanotechnology, 2017, 28, 425102.	1.3	12
154	A cancer cell specific targeting nanocomplex for combination of mRNA-responsive photodynamic and chemo-therapy. Chemical Communications, 2017, 53, 9979-9982.	2.2	15
155	Long-term adefovir therapy may induce Fanconi syndrome: A report of four cases. Experimental and Therapeutic Medicine, 2017, 14, 424-430.	0.8	3
156	Reveal the molecular signatures of hepatocellular carcinoma with different sizes by iTRAQ based quantitative proteomics. Journal of Proteomics, 2017, 150, 230-241.	1.2	10
157	The hepatectomy efficacy of huge hepatocellular carcinoma and its risk factors. Medicine (United) Tj ETQq1 1 0	.784314 r 0.4	gBT_/Overloc 14
158	Smart Cu(II)-aptamer complexes based gold nanoplatform for tumor micro-environment triggered programmable intracellular prodrug release, photodynamic treatment and aggregation induced photothermal therapy of hepatocellular carcinoma. Theranostics, 2017, 7, 164-179.	4.6	69
159	Coexpression Analysis of Transcriptome on AIDS and Other Human Disease Pathways by Canonical Correlation Analysis. International Journal of Genomics, 2017, 2017, 1-10.	0.8	1
160	Adipose tissue-derived stem cells ameliorate hyperglycemia, insulin resistance and liver fibrosis in the type 2 diabetic rats. Stem Cell Research and Therapy, 2017, 8, 286.	2.4	22
161	DAPK1 as an independent prognostic marker in liver cancer. PeerJ, 2017, 5, e3568.	0.9	23
162	The influence of house dust mite sublingual immunotherapy on the TSLPâ€OX40L signaling pathway in patients with allergic rhinitis. International Forum of Allergy and Rhinology, 2016, 6, 862-870.	1.5	20

#	Article	IF	CITATIONS
163	One-pot synthesis of gold nanostars using plant polyphenols for cancer photoacoustic imaging and photothermal therapy. Journal of Nanoparticle Research, 2016, 18, 1.	0.8	20
164	The application of proteomics in different aspects of hepatocellular carcinoma research. Journal of Proteomics, 2016, 145, 70-80.	1.2	20
165	A highly stable and biocompatible optical bioimaging nanoprobe based on carbon nanospheres. RSC Advances, 2016, 6, 37472-37477.	1.7	3
166	SPION@Cu _{2â^'x} S nanoclusters for highly sensitive MRI and targeted photothermal therapy of hepatocellular carcinoma. Journal of Materials Chemistry B, 2016, 4, 4119-4129.	2.9	18
167	Peroxidase-like catalytic activity of copper ions and its application for highly sensitive detection of glypican-3. Analytica Chimica Acta, 2016, 941, 87-93.	2.6	23
168	Adipose tissue-derived stem cells promote the reversion of non-alcoholic fatty liver disease: An in vivo study. International Journal of Molecular Medicine, 2016, 37, 1389-1396.	1.8	14
169	Poly (dopamine) coated superparamagnetic iron oxide nanocluster for noninvasive labeling, tracking and targeted delivery of adipose tissue-derived stem cells. Scientific Reports, 2016, 6, 18746.	1.6	39
170	Long non-coding RNA linc-cdh4-2 inhibits the migration and invasion of HCC cells by targeting R-cadherin pathway. Biochemical and Biophysical Research Communications, 2016, 480, 348-354.	1.0	16
171	Lipid micelles packaged with semiconducting polymer dots as simultaneous MRI/photoacoustic imaging and photodynamic/photothermal dual-modal therapeutic agents for liver cancer. Journal of Materials Chemistry B, 2016, 4, 589-599.	2.9	75
172	Magnetite nanocluster@poly(dopamine)-PEG@ indocyanine green nanobead with magnetic field-targeting enhanced MR imaging and photothermal therapy in vivo. Colloids and Surfaces B: Biointerfaces, 2016, 141, 467-475.	2.5	52
173	Intrahepatic transplantation of adipose-derived stem cells attenuates the progression of non-alcoholic fatty liver disease in rats. Molecular Medicine Reports, 2015, 12, 3725-3733.	1.1	22
174	Dataset for the quantitative proteomics analysis of the primary hepatocellular carcinoma with single and multiple lesions. Data in Brief, 2015, 5, 226-240.	0.5	7
175	Highly efficient loading of doxorubicin in Prussian Blue nanocages for combined photothermal/chemotherapy against hepatocellular carcinoma. RSC Advances, 2015, 5, 30970-30980.	1.7	41
176	Nanocluster of superparamagnetic iron oxide nanoparticles coated with poly (dopamine) for magnetic field-targeting, highly sensitive MRI and photothermal cancer therapy. Nanotechnology, 2015, 26, 115102.	1.3	136
177	Chlorin e6 Conjugated Poly(dopamine) Nanospheres as PDT/PTT Dual-Modal Therapeutic Agents for Enhanced Cancer Therapy. ACS Applied Materials & Interfaces, 2015, 7, 8176-8187.	4.0	311
178	Horseradish peroxidase and aptamer dual-functionalized nanoprobe for the amplification detection of alpha-methylacyl-CoA racemase. Analytica Chimica Acta, 2015, 899, 100-105.	2.6	10
179	Comparative analysis of primary hepatocellular carcinoma with single and multiple lesions by iTRAQ-based quantitative proteomics. Journal of Proteomics, 2015, 128, 262-271.	1.2	21
180	Multifunctional PEG modified DOX loaded mesoporous silica nanoparticle@CuS nanohybrids as photo-thermal agent and thermal-triggered drug release vehicle for hepatocellular carcinoma treatment. Nanotechnology, 2015, 26, 025102.	1.3	54

#	Article	IF	CITATIONS
181	Prevalence and Clinical Relevance of T-Helper Cells, Th17 and Th1, in Hepatitis B Virus-Related Hepatocellular Carcinoma. PLoS ONE, 2014, 9, e96080.	1.1	40
182	α-Methylacyl-CoA racemase (AMACR) serves as a prognostic biomarker for the early recurrence/metastasis of HCC. Journal of Clinical Pathology, 2014, 67, 974-979.	1.0	15
183	Coexpression within Integrated Mitochondrial Pathways Reveals Different Networks in Normal and Chemically Treated Transcriptomes. International Journal of Genomics, 2014, 2014, 1-10.	0.8	4
184	Lipid-AuNPs@PDA Nanohybrid for MRI/CT Imaging and Photothermal Therapy of Hepatocellular Carcinoma. ACS Applied Materials & Interfaces, 2014, 6, 14266-14277.	4.0	151
185	Quantitative proteomics analysis of early recurrence/metastasis of huge hepatocellular carcinoma following radical resection. Proteome Science, 2014, 12, 22.	0.7	36
186	Preliminary Estimation of Rotary Torque Produced by Proton-Motive Force in Fully Functional FOF1-ATPase. Protein and Peptide Letters, 2007, 14, 45-50.	0.4	1
187	Using giant unilamellar lipid vesicle micro-patterns as ultrasmall reaction containers to observe reversible ATP synthesis/hydrolysis of FOF1-ATPase directly. Biochimica Et Biophysica Acta - General Subjects, 2007, 1770, 1620-1626.	1.1	6